FEBS Letters 587 (2013) 569–574

FEBS Letters

journal homepage: www.FEBSLetters.org

Identification of a novel 'aggregation-prone'/'amyloidogenic determinant' peptide in the sequence of the highly amyloidogenic human calcitonin

Vassiliki A. Iconomidou [a], Aristeidis Leontis [a], Andreas Hoenger [b,1], Stavros J. Hamodrakas [a,*]

[a] Department of Cell Biology and Biophysics, Faculty of Biology, University of Athens, Panepistimiopolis, Athens 157 01, Greece
[b] University of Colorado at Boulder, Department of Molecular, Cellular and Developmental Biology, Boulder, CO 80309-0347, USA

ARTICLE INFO

Article history:
Received 2 December 2012
Revised 7 January 2013
Accepted 14 January 2013
Available online 8 February 2013

Edited by Jesus Avila

Keywords:
Human calcitonin
Amyloid fibril
Osteoporosis
Medullary thyroid carcinoma

ABSTRACT

Calcitonin is a 32-residue polypeptide hormone, which takes part in calcium metabolism in bones. It may form amyloid fibrils. Amyloid fibrils are related with serious diseases known as amyloidoses. The amyloid form of calcitonin takes part in medullary thyroid carcinoma. A novel hexapeptide (^{6}TCMLGT^{11}) of human calcitonin was predicted as a possible 'aggregation-prone' peptide, which may play a role in amyloid formation. We investigated experimentally the ability of an analog of this hexapeptide (cysteine replaced by alanine, TAMLGT) to form amyloid fibrils utilizing TEM, X-ray fiber diffraction, ATR FT-IR spectroscopy, and polarized light microscopy. This peptide self-assembles into amyloid-like fibrils and fibrillogenesis is mediated via nuclei of liquid crystalline nature, known as spherulites.

Structured summary of protein interactions:
TAMLGT peptide and **TAMLGT peptide**bind by x-ray fiber diffraction (View interaction)
TAMLGT peptide and **TAMLGT peptide**bind by infrared spectroscopy (View interaction)
TAMLGT peptide and **TAMLGT peptide**bind by electron microscopy (View interaction)

1. Introduction

A great number of proteins and peptides with different functions and various structures are grouped together because of their ability to form ordered fibrillar aggregates, known as amyloid fibrils. These fibrils share distinct, common features: they bind Congo Red and display a characteristic yellow-green birefringence under polarized light [1], they are seen, utilizing electron microscopy, as uniform, straight or slightly curved, unbranched and of indefinite length fibrils, approximately 100 Å in diameter [2], and, finally they produce cross-β X-ray fiber diffraction patterns [3–5]. Amyloid fibrils are related to diseases, such as Alzheimer's disease, atherosclerosis, cerebral amyloid angiopathy (Icelandic type), type II diabetes, medullary thyroid carcinoma, which are, collectively, called amyloidoses [6]. However, there are cases where certain proteins or peptides with an amyloid-forming potency play important functional roles in some organisms, including insects [4], bacteria [7] and even humans [8].

Calcitonin, a 32-amino acid polypeptide hormone [9] (Fig. 1), is produced in mammals by the C-cells of the thyroid gland and in lower vertebrates by the ultimobranchial body [10]. This hormone (hereinafter called also hCT from human CalciTonin) is involved in calcium-phosphorus metabolism [10]. Therefore, it is used as a drug to treat various bone disorders like postmenopausal osteroposis [11], Paget's disease [12] and also for short-term management of severe symptomatic hypercalcaemia [13]. It has been found that deposition of full-length calcitonin amyloid fibrils is associated with medullary thyroid carcinoma [14,15]. More specifically it has been proved that full-length calcitonin hormone and not an alternatively processed prohormone of calcitonin, forms amyloid in medullary thyroid carcinoma [16]. It has also been found that human calcitonin (hCT) may aggregate in vitro under specific incubation conditions. Many studies have been done about the mechanisms and kinetics of calcitonin fibrillation [17,18].

It has been shown that five residues corresponding to positions 15–19 of hCT (DFNKF) play an active role in oligomerisation and fibril formation by hCT in vitro [19], and Lys-18 and Phe-19 have been identified as key residues in both the bioactivity and self-assembly of hCT [20]. Attempts were also made to convert the highly amyloidogenic hCT into a powerful fibril inhibitor by three-dimensional structure homology with a non-amyloidogenic

* Corresponding author. Fax: +30 210 7274254.
E-mail addresses: veconom@biol.uoa.gr (V.A. Iconomidou), arisleontis@hotmail.com (A. Leontis), Andreas.Hoenger@Colorado.edu (A. Hoenger), shamodr@biol.uoa.gr (S.J. Hamodrakas).
[1] Fax: +1 303 7350770.

0014-5793/$36.00
http://dx.doi.org/10.1016/j.febslet.2013.01.031

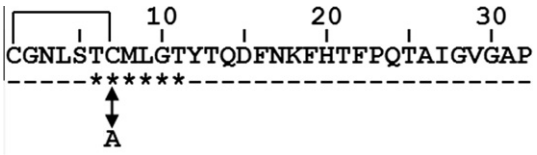

Fig. 1. A schematic representation of the aminoacid sequence of mature human calcitonin (hCT), which consists of 32 amino acid residues, is shown. There is a disulfide bridge between Cys1 and Cys7 in mature calcitonin, essential for its biological action, which is depicted by straight lines connecting the two residues, above the sequence. A predicted 'amyloidogenic determinant'/'aggregation-prone' peptide (^{6}TCMLGT^{11}) by our algorithm AMYLPRED [23] is marked by "$*$" (asterisks) below the sequence. An analog of this peptide (^{6}TAMLGT^{11}), by replacing cysteine (C) with alanine (A) (double arrow), was synthesized and studied in this work. This peptide was also predicted to be 'amyloidogenic determinant'/'aggregation-prone' by AMYLPRED [23].

analog [21], and, also to rationally design an aggregation-resistant bioactive calcitonin [22].

AMYLPRED is a consensus prediction algorithm for amyloid fibril favoring regions, the so-called amyloidogenic determinants/'aggregation-prone' stretches, which was produced in our lab and is freely available for academic users at http://biophysics.biol.uoa.gr/AMYLPRED [23]. Testing the hCT sequence by AMYLPRED, the hexapeptide TCMLGT (residues 6–11 of the protein), was predicted as a possible amyloidogenic determinant/'aggregation-prone' sequence. We synthesized an analog of this peptide by replacing cysteine with alanine in order to prevent the formation of intermolecular disulfide bonds between cysteines, at approximately the neutral pH we wanted to perform the experiments. We should note that, the 'mutant' peptide TAMLGT was predicted by AMYLPRED as an 'aggregation-prone' peptide as well, in the 'mutated' calcitonin sequence.

In this work, the hexapeptide TAMLGT was tested experimentally for fulfilling the criteria stated above, to see whether it is capable of forming amyloid fibrils or not. It will be shown below that the tests were positive and that this hexapeptide self-assembles to form amyloid fibrils, via nuclei of liquid crystalline nature, known as spherulites [24]. The fact that nuclei (spherulites) with a liquid crystalline texture act as pre-fibrillar intermediates in amyloid fibril formation, has been observed in several other peptide or protein systems forming amyloid fibrils [24].

2. Materials and methods

2.1. Peptide synthesis

The TAMLGT peptide was synthesized by GeneCust Europe, Luxembourg (purity >98%, free N- and C-terminals).

2.2. Formation of amyloid-like fibrils

The synthesized TAMLGT peptide was dissolved in doubly distilled water (pH 5.5), at a concentration of 15 mg ml^{-1}. Mature amyloid-like fibrils were formed after 1–2 weeks incubation at ambient (room) temperatures, forming a fibril-containing gel. The fibrils were judged to be mature, observing preparations both for shorter and longer periods than 1–2 weeks. Oriented fibers, suitable for X-ray diffraction, were obtained from solutions of the peptide, containing mature amyloid-like fibrils as described below.

2.3. X-ray diffraction

A droplet (~10 μl) of mature fibril suspension was placed between two siliconized glass rods, spaced ~1.5 mm apart and mounted horizontally on a glass substrate, as collinearly as possible. The droplet was allowed to dry slowly at ambient temperature and humidity for 1 h to form an oriented fiber suitable for X-ray diffraction. X-ray patterns were obtained immediately from these fibers since it was found that fibers were drying and destroyed, after ~2 h under these conditions. X-ray diffraction patterns were recorded on a Mar Research 345 mm image plate, utilizing Cu Kα radiation (λ = 1.5418 Å), obtained from a Rigaku MicroMax-007 HF, microfocus rotating anode generator (with Osmic Rigaku VariMax™ HF optics), operating at 40 kV, 20 mA. The specimen-to-film distance was set at 150 mm and the exposure time was 30 min. No additional low angle reflections were observed at longer specimen-to-film distances, up to 300 mm. The X-ray patterns, initially viewed using the program MarView (MAR Research, Hamburg, Germany), were displayed and measured with the aid of the program IPDISP of the CCP4 package [25].

2.4. Negative staining

For negative staining, the TAMLGT peptide fibril suspensions were applied to glow-discharged 400 mesh carbon coated copper grids for 60 s. The grids were (occasionally) flash-washed with ~150 μl of distilled water and stained with a drop of 1% (w/v) aqueous uranyl acetate for 45 s. Excess stain was removed by blotting with a filter paper and the grids were air-dried. Pictures were acquired in a Philips CM120 BioTWIN electron microscope (FEI, Eindoven, The Netherlands) operating at 100 kV. Digital acquisitions were made with a bottom-mounted Keen View 1K CCD camera (Soft Imaging System, Muenster, Germany).

2.5. Congo Red staining and polarized light microscopy

TAMLGT fibril suspensions were applied to glass slides and stained with a 10 mM Congo Red (Sigma) solution in phosphate-buffered saline (pH 7.4) for approximately 2 h. They were then washed several times with 90% ethanol and left to dry. The samples were observed respectively, both under bright field illumination and between crossed polars using a Leica MZ75 polarizing stereomicroscope equipped with a JVC GC-X3E camera.

2.6. Attenuated total reflectance Fourier-transform infrared (ATR FT-IR) spectroscopy and post-run computations of the spectra

Ten microliter drops of the TAMLGT peptide suspension (Section 2.2) were cast on flat stainless-steel plates, coated with an ultra thin hydrophobic layer (SpectRIM, Tienta Sciences, Inc. Indianapolis, USA) and left to air-dry slowly at ambient conditions to form thin films. IR spectra were obtained from these films, at a resolution of 4 cm^{-1}, utilizing an IR microscope (IRScope II, Bruker Optik GmbH, Ettlingen, Germany), equipped with a Ge ATR objective lens (20×) and attached to a FT-IR spectrometer (Equinox 55, Bruker Optik GmbH, Ettlingen, Germany). Ten 32-scan spectra were collected from each sample and averaged to improve the S/N ratio. Internal reflection spectroscopy has several advantages compared to the more common KBr dispersion technique [26]. The choice of ATR was dictated by the need to exclude any possible spectroscopic and chemical interactions between the sample and the dispersing medium. Having a penetration depth of less than 1 μm (1000 cm^{-1}, Ge), ATR is free of saturation effects, which may be present in the transmission spectra of thicker samples. The spectra were corrected for the effect of wavelength on the penetration depth (p.d. $\propto \lambda$). The corresponding effect of the (frequency-dependent) refractive index (n) of the samples was not taken into account due to the lack of relevant data.

The infrared ATR band maxima were determined from the minima in the second derivative of the corresponding spectra. Derivatives were computed analytically using routines of the Bruker

OPUS/OS2 software and included smoothing by the Savitsky-Golay algorithm [27] over a ±8 cm^{-1} range, around each data point. Smoothing over narrower ranges resulted in a deterioration of the signal-to-noise ratio and did not increase the number of minima that could be determined with confidence.

2.7. Crystalization experiments and polarized light microscopy

Quantities of freshly made peptide solutions in distilled water (concentration 1 mg ml^{-1}, pH 5.5) were tested in crystallization experiments, using the "hanging-drop" method, for the possible formation of crystals. The precipitant was $(NH_4)_2SO_4$ (concentration varied from 1.0 to 2.0 M). The samples were observed, both under bright field illumination and between crossed polars, respectively, using a Leica MZ75 polarizing stereomicroscope equipped with a JVC GC-X3E camera.

3. Results and discussion

The synthesized peptide (TAMLGT) self-assembles into amyloid-like fibrils, after 1–2 week incubation in distilled water (see Section 2) and forms a fibril-containing gel. The fibrils were judged to be amyloid-like from their tinctorial and structural characteristics. Transmission electron microscopy (negative staining) shows that the fibrils are straight, unbranched and of indeterminable length (Fig. 2A and B). Each fibril/protofilament is about 40–50 Å in diameter. Non-twisted ribbons/tapes were observed, as a result of lateral interactions between multiple protofilaments. Similar ribbons/tapes have been observed in amyloid fibrils from human calcitonin [18]. The similarity is astonishing and it might imply that this peptide plays a crucial role in human calcitonin fibrillation. Future attempts for preventing hCT fibrillation and producing more effective drugs, should perhaps target this region of the molecule. While preparing peptide solutions, gels were quickly formed, implying the existence of interacting amyloid fibrils (data not shown).

Fibers of TAMLGT fibrils give an X-ray diffraction pattern (Fig. 3), which closely resembles the typical "cross-β" patterns taken from oriented amyloid fibers. However, the X-ray diffraction pattern is not a typical "cross-β" pattern, since, instead of oriented reflections at the meridian and the equator, it shows rings. This indicates a powder-like pattern of a polycrystalline material. Nevertheless, it can easily be explained by looking at the EM photographs of Fig. 2, assuming that the ribbons/tapes of the fibrils, adopt all possible orientations in our attempts to obtain an oriented fiber. A full explanation of the diffraction pattern is given in the legend to Table 1, with a table of the d-spacings of the diffraction rings and a proposed unit cell for the polycrystalline fiber.

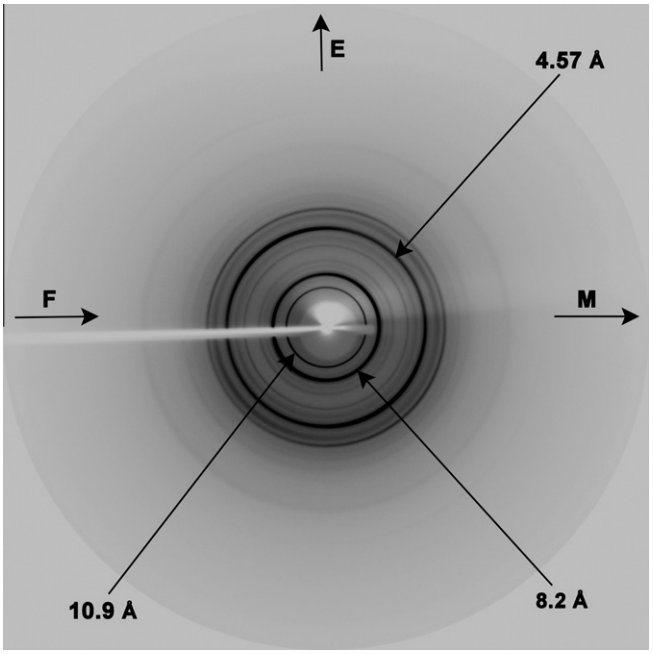

Fig. 3. X-ray diffraction pattern from an oriented fiber (F) of TAMLGT peptide amyloid-like fibrils. The meridian, M (direction parallel to the fiber axis) is horizontal and the equator, E, is vertical, in this display. The X-ray diffraction pattern is not a typical "cross-β" pattern since it shows rings instead of oriented relections at the meridian and the equator. This, indicates a powder-like pattern of a polycrystalline material. Nevertheles, it can easily be explained by looking at the EM photographs of Fig. 2, assuming that the ribbons of the fibrils, adopt all possible orientations, despite our attempts to obtain an oriented fiber. A full explanation of the diffraction pattern is given in the text, with a table of the d-spacings of the diffraction rings and a proposed unit cell for the polycrystalline fiber (Table 1). However, the typical to "cross-β", 4.57 Å and 10.9 Å reflections are seen. The 4.57 Å reflection corresponds to the spacing of adjacent beta-strands (which should be perpendicular to the fiber axis, and, consequently, the reflection perpendicular to the meridian, in a typical "cross-β" structure), and the 10.9 Å spacing, which corresponds to the face-to-face separation (packing distance) of the β-sheets.

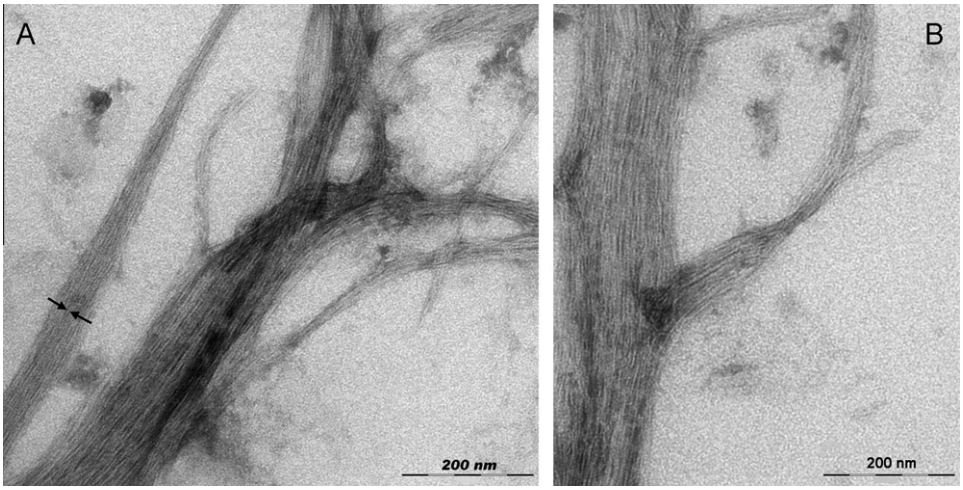

Fig. 2. Electron micrographs (A & B) of mature TAMLGT peptide amyloid-like fibrils, derived after 1–2 weeks of incubation. The fibrils are seen to assemble laterally to form ribbons, in many ways reminiscent of the fibrils and ribbons formed by the entire calcitonin molecule [18]. The similarity in size of the fibrils and appearance of the ribbons is, indeed, intriguing. The samples were negatively stained with 1% uranyl acetate. Arrows show the width of a fibril (40–50 Å). Bar 200 nm.

Table 1
Spacings (d_{obs}) of the reflections observed in the X-ray diffraction pattern, taken from a fiber of the ^{6}TAMLGT^{11} peptide amyloid-like fibrils (Fig. 3). Indexing (h, k, l, d_{obs}, d_{calc}) was done, utilizing DICVOL06 [38], a software for the automatic indexing of powder diffraction patterns by the successive dichotomy method, based on an orthorhombic unit cell, with unit cell parameters: a = 18.30 ± 0.02 Å, b = 18.53 ± 0.01 Å, c = 21.79 ± 0.01 Å, $\alpha = 90°$, $\beta = 90°$, $\gamma = 90°$. This unit cell has a volume, Vol = 7388.96 ± 0.02 Å^3 and it is estimated to contain 8 molecules of TAMLGT, together with 8 associated water molecules.

h	k	l	d_{obs} (Å)	d_{calc} (Å)
0	0	2	10.90	10.89
2	1	0	8.20	8.20
0	0	3	7.25	7.26
1	2	2	6.58	6.58
2	1	3	5.45	5.44
1	2	3		5.45
0	0	4		5.45
3	2	1	4.96	4.96
4	0	0	4.57	4.57
4	2	0	4.10	4.10
4	0	3	3.87	3.87
0	5	0	3.70	3.70
0	5	2	3.51	3.51
0	5	3	3.30	3.30
4	2	6	2.72	2.72
0	0	8		2.72
2	7	3	2.40	2.40
5	4	5		2.40
4	5	5		2.40
3	2	8		2.40
1	0	9		2.40
0	1	9		2.40

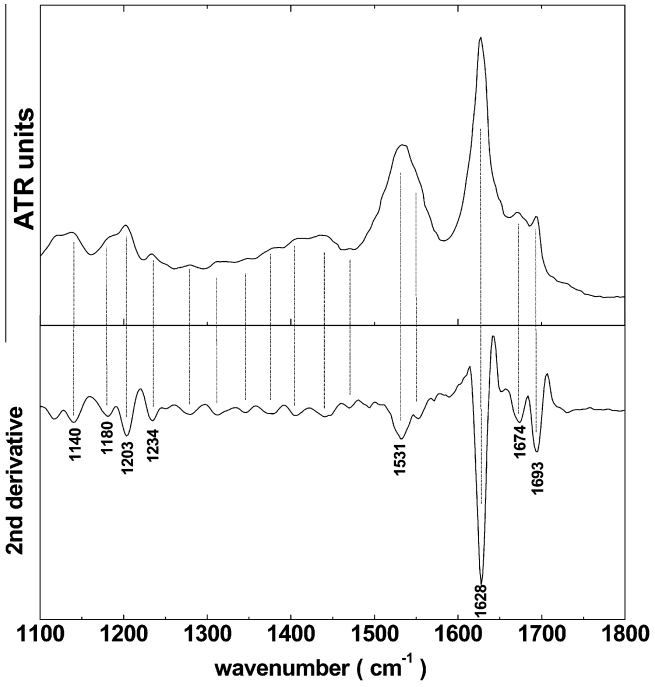

Fig. 4. ATR FT-IR (900–1800 cm^{-1}) spectrum of TAMLGT peptide amyloid fibrils, cast on a flat stainless-steel plate, coated with an ultra thin hydrophobic layer (SpectRIM, Tienta Sciences, Inc. Indianapolis, USA) and left to air-dry slowly, at ambient conditions, to form a hydrated, thin film. A second derivative spectrum is also included.

Nevertheless, the typical to a "cross-β" structure, 4.57 Å and 10.9 Å reflections are seen. The structural repeat of 4.57 Å along the fiber axis corresponds to the spacing of adjacent beta-strands (which should be perpendicular to the fiber axis, in a typical "cross-β" structure) and the 10.9 Å spacing, which corresponds to the face-to-face separation (packing distance) of the β-sheets, parallel to the fiber axis in typical cross-β patterns.

Table 2
Bands observed in an ATR FT-IR spectrum taken from a thin hydrated film, formed from the hCT hexapeptide-analog, TAMLGT, amyloid-like fibril suspension, cast on a flat stainless-steel plate, coated with an ultra thin hydrophobic layer (SpectRIM, Tienta Sciences, Inc. Indianapolis, USA), and their tentative assignments (see Section 2).

Band (cm^{-1})	Assignment
1140	TFA
1180	TFA
1203	TFA
1234	Amide III (β-sheet)
1531	Amide II (β-sheet)
1628	Amide I (β-sheet)
1674	TFA
1693	Amide I (antiparallel β-sheet)

The ATR FT-IR spectrum of the TAMLGT peptide fibrils, cast as a thin-hydrated film, is shown in Fig. 4. The spectrum shows a prominent band at 1628 cm^{-1} in the amide I region and the amide III band at 1234 cm^{-1}, which are both definitely due to β-sheet conformation [28–32]. The amide I, high wavenumber component at 1693 cm^{-1} is a strong indication that the β-sheets are antiparallel [29–32]. In proteins containing antiparallel β-sheets, a high frequency β-sheet component that arises from transition dipole coupling is usually found 50–70 cm^{-1} higher than the main β-sheet component [31]. Other ATR FT-IR bands and their tentative assignments are shown in Table 2. Thus, the results from ATR FT-IR spectroscopy strongly support the evidence from X-ray diffraction.

Also, the fibrils formed from the TAMLGT peptide, bind the dye Congo Red showing the characteristic green-yellow/green birefringence when viewed under crossed polars in a polarizing microscope (Fig. 5).

Immediately after dissolving the peptide TAMLGT in distilled water or during our attempts to crystallize it (see Section 2), having seen from the X-ray diffraction experiments that it has a polycrystalline texture, it was found that the peptide spontaneously assembles into supramolecular spherical structures, after 1–2 h incubation, under a great variety of conditions. These structures, when viewed in a polarizing microscope under crossed polars, are seen to have a liquid crystalline texture. They are spherulites

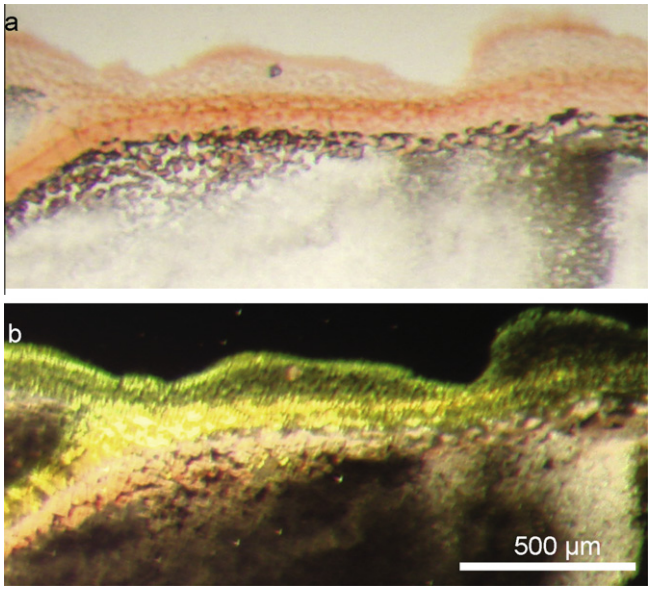

Fig. 5. Photomicrographs of TAMLGT peptide fibrils stained with Congo Red: (a) bright field illumination, (b) crossed polars. The yellow-green birefringence characteristic for amyloid fibrils is clearly seen. Bar 500 μm.

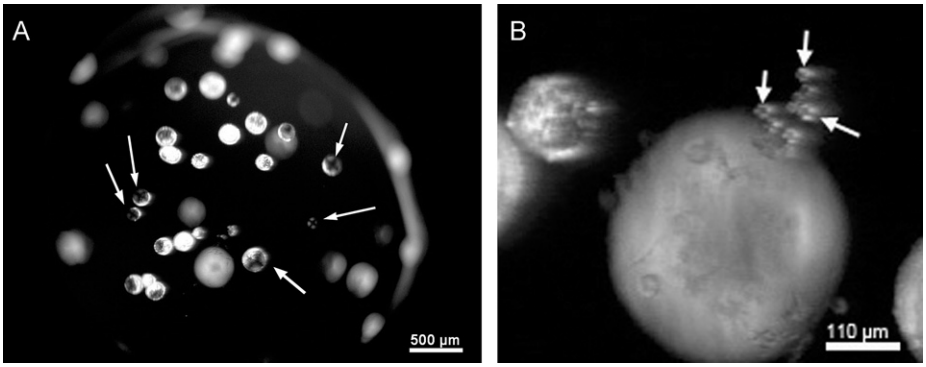

Fig. 6. Photomicrographs of TAMLGT peptide spherulites viewed in a polarizing microscope under crossed polars (A and B). These supramolecular spherical structures, with a liquid crystalline texture, are formed spontaneously after 2–4 h incubation, under a great variety of conditions. Characteristic "Maltese extinction crosses" are clearly seen (arrows). The spherulites appear to have diameters ranging from 10 to 200 μm. (A) Bar 500 μm, (B) bar 110 μm.

with "Maltese crosses". The spherulites appear to have diameters ranging from 10 to 200 μm (Fig. 6A and B).

These liquid crystalline structures can be found in many other amyloid-fibril forming proteins [24,33–36]. Thus, amyloid fibrillogenesis proceeds via spherulites for proteins and peptides involved in functional amyloids like silkmoth chorion and spider silk and pathological amyloids ($A\beta_{42}$ involved in Alzheimer's disease) [24,35 and references therein] and for insulin, albumin, β-lactoglobulin and pro-IAPP [34–36 and references therein]. Spherulites have also been found in vivo, in the hippocampal tissue, in Alzheimer's disease [33]. Therefore, it is tempting to assume that amyloid fibrillogenesis proceeds, in several cases via intermediates of liquid crystalline nature, a fact initially recognized by our team findings [24] and that, in several cases, the pre-fibrillar amyloid intermediates, important for the pathogenicity in amyloidoses are, indeed, these spherulitic structures.

At this point, it is perhaps interesting to draw attention to the relation of spherulites (as ordered domains of hydrogels) to the general theory of formation of hydrogels, which may be formed by different types of synthetic polymers [37 and references therein]. A full understanding of the process that leads from spherulites to amyloid fibrils, is likely to lead not just to advances in our understanding of amyloid diseases and the formation of functional amyloids, but also to a fundamental understanding of assembly characteristics, for possible exploitation in the generation of novel biomaterials and in nanotechnology.

Our future attempts (in progress) will be focused to produce more soluble/effective variants of hCT, designing non-fibrillating mutants of calcitonin, by performing mutations in this part of hCT, involving this peptide.

Acknowledgements

We should like to thank Peter Everitt for excellent technical assistance and continuous unfailing help and EMBL, Heidelberg for hospitality. We thank the University of Athens for support. We also thank the Cooperation 2011 program (11SYN_1_1230) of the General Secretariat for Research and Technology of the Greek Ministry of Education and Religious Affairs, Culture and Sports, under the NSRF 2007–2013, for financial support. We should also like to thank the editor of this manuscript for properly handling it and the anonymous reviewers for useful and constructive criticism.

References

[1] Glenner, G.G., Eanes, E.D. and Page, D.L. (1972) The relation of the properties of Congo red-stained amyloid fibrils to the β-conformation. J. Histochem. Cytochem. 20, 821–826.
[2] Shirahama, T. and Cohen, A.S. (1965) Structure of amyloid fibrils after negative staining and high-resolution electron microscopy. Nature 206, 737–738.
[3] Geddes, A.J., Parker, K.D., Atkins, E.D. and Beighton, E. (1968) "Cross-beta" conformation in proteins. J. Mol. Biol. 32, 343–358.
[4] Iconomidou, V.A., Vriend, G. and Hamodrakas, S.J. (2000) Amyloids protect the silkmoth oocyte and embryo. FEBS Lett. 479, 141–145.
[5] Sunde, M. and Blake, C. (1997) The structure of amyloid fibrils by electron microscopy and X-ray diffraction. Adv. Protein Chem. 50, 123–159.
[6] Fandrich, M. (2007) On the structural definition of amyloid fibrils and other polypeptide aggregates. Cell Mol. Life Sci. 64, 2066–2078.
[7] Chapman, M.R., Robinson, L.S., Pinkner, J.S., Roth, R., Heuser, J., Hammar, M., Normark, S. and Hultgren, S.J. (2002) Role of *Escherichia coli* curli operons in directing amyloid fiber formation. Science 295, 851–855.
[8] Fowler, D.M., Koulov, A.V., Balch, W.E. and Kelly, J.W. (2007) Functional amyloid—from bacteria to humans. Trends Biochem. Sci. 32, 217–224.
[9] Copp, D.H. and Cheney, B. (1962) Calcitonin—a hormone from the parathyroid which lowers the calcium-level of the blood. Nature 193, 381–382.
[10] Kleeman, C.R., Massry, S.G. and Coburn, J.W. (1971) The clinical physiology of calcium homeostasis, parathyroid hormone, and calcitonin. I. Calif. Med. 114, 16–43.
[11] Chatziavramidis, A., Mantsopoulos, K., Gennadiou, D. and Sidiras, T. (2008) Intranasal complications in women with osteoporosis under treatment with nasal calcitonin spray: case reports and review of the literature. Auris Nasus Larynx 35, 417–422.
[12] Gagel, R.F., Logan, C. and Mallette, L.E. (1988) Treatment of Paget's disease of bone with salmon calcitonin nasal spray. J. Am. Geriatr. Soc. 36, 1010–1014.
[13] Altmann, P. and Cunningham, J. (1987) The management of severe hypercalcaemia. Postgrad. Med. J. 63, 77–79.
[14] Hazard, J.B., Hawk, W.A. and Crile Jr., G. (1959) Medullary (solid) carcinoma of the thyroid; a clinicopathologic entity. J. Clin. Endocrinol. Metab. 19, 152–161.
[15] Williams, E.D. (1966) Histogenesis of medullary carcinoma of the thyroid. J. Clin. Pathol. 19, 114–118.
[16] Khurana, R., Agarwal, A., Bajpai, V.K., Verma, N., Sharma, A.K., Gupta, R.P. and Madhusudan, K.P. (2004) Unraveling the amyloid associated with human medullary thyroid carcinoma. Endocrinology 145, 5465–5470.
[17] Arvinte, T., Cudd, A. and Drake, A.F. (1993) The structure and mechanism of formation of human calcitonin fibrils. J. Biol. Chem. 268, 6415–6422.
[18] Bauer, H.H., Aebi, U., Haner, M., Hermann, R., Muller, M. and Merkle, H.P. (1995) Architecture and polymorphism of fibrillar supramolecular assemblies produced by in vitro aggregation of human calcitonin. J. Struct. Biol. 115, 1–15.
[19] Reches, M., Porat, Y. and Gazit, E. (2002) Amyloid fibril formation by pentapeptide and tetrapeptide fragments of human calcitonin. J. Biol. Chem. 277, 35475–35480.
[20] Kazantzis, A., Waldner, M., Taylor, J.W. and Kapurniotu, A. (2002) Conformationally constrained human calcitonin (hCt) analogues reveal a critical role of sequence 17–21 for the oligomerization state and bioactivity of hCt. Eur. J. Biochem. 269, 780–791.
[21] Andreotti, G., Vitale, R.M., Avidan-Shpalter, C., Amodeo, P., Gazit, E. and Motta, A. (2011) Converting the highly amyloidogenic human calcitonin into a powerful fibril inhibitor by three-dimensional structure homology with a non-amyloidogenic analogue. J. Biol. Chem. 286, 2707–2718.
[22] Fowler, S.B., Poon, S., Muff, R., Chiti, F., Dobson, C.M. and Zurdo, J. (2005) Rational design of aggregation-resistant bioactive peptides: reengineering human calcitonin. Proc. Natl. Acad. Sci. USA 102, 10105–10110.
[23] Frousios, K.K., Iconomidou, V.A., Karletidi, C.M. and Hamodrakas, S.J. (2009) Amyloidogenic determinants are usually not buried. BMC Struct. Biol. 9, 44.
[24] Hamodrakas, S.J., Hoenger, A. and Iconomidou, V.A. (2004) Amyloid fibrillogenesis of silkmoth chorion protein peptide-analogues via a liquid-crystalline intermediate phase. J. Struct. Biol. 145, 226–235.
[25] Winn, M.D. et al. (2011) Overview of the CCP4 suite and current developments. Acta Crystallogr. D Biol. Crystallogr. 67, 235–242.
[26] de Jongh, H.H., Goormaghtigh, E. and Ruysschaert, J.M. (1996) The different molar absorptivities of the secondary structure types in the amide I region: an attenuated total reflection infrared study on globular proteins. Anal. Biochem. 242, 95–103.

[27] Savitsky, A. and Golay, M.J.E. (1964) Smoothing and differentiation of data by simplified least-squares procedures. Analytical Chemistry 36, 1627–1639.
[28] Surewicz, W.K., Mantsch, H.H. and Chapman, D. (1993) Determination of protein secondary structure by Fourier transform infrared spectroscopy: a critical assessment. Biochemistry 32, 389–394.
[29] Cai, S. and Singh, B.R. (1999) Identification of beta-turn and random coil amide III infrared bands for secondary structure estimation of proteins. Biophys. Chem. 80, 7–20.
[30] Haris, P.I. and Chapman, D. (1995) The conformational analysis of peptides using Fourier transform IR spectroscopy. Biopolymers 37, 251–263.
[31] Jackson, M. and Mantsch, H.H. (1995) The use and misuse of FTIR spectroscopy in the determination of protein structure. Crit. Rev. Biochem. Mol. Biol. 30, 95–120.
[32] Krimm, S. and Bandekar, J. (1986) Vibrational spectroscopy and conformation of peptides, polypeptides, and proteins. Adv. Protein Chem. 38, 181–364.
[33] Exley, C., House, E., Collingwood, J.F., Davidson, M.R., Cannon, D. and Donald, A.M. (2010) Spherulites of amyloid-beta42 in vitro and in Alzheimer's disease. J. Alzheimers Dis. 20, 1159–1165.
[34] Exley, C., House, E., Patel, T., Wu, L. and Fraser, P.E. (2010) Human pro-islet amyloid polypeptide (ProIAPP(1–48)) forms amyloid fibrils and amyloid spherulites in vitro. J. Inorg. Biochem. 104, 1125–1129.
[35] Krebs, M.R., Macphee, C.E., Miller, A.F., Dunlop, I.E., Dobson, C.M. and Donald, A.M. (2004) The formation of spherulites by amyloid fibrils of bovine insulin. Proc. Natl. Acad. Sci. USA 101, 14420–14424.
[36] Rogers, S.S., Krebs, M.R., Bromley, E.H., van der Linden, E. and Donald, A.M. (2006) Optical microscopy of growing insulin amyloid spherulites on surfaces in vitro. Biophys. J. 90, 1043–1054.
[37] Berger, J., Reist, M., Mayer, J.M., Felt, O. and Gurny, R. (2004) Structure and interactions in chitosan hydrogels formed by complexation or aggregation for biomedical applications. Eur. J. Pharm. Biopharm. 57, 35–52.
[38] Boultif, A. and Louër, D. (2004) Powder pattern indexing with the dichotomy method. J. Appl. Cryst. 37, 724–731.